

Guided ion beam studies of the reactions of Cr_n^+ ($n=1-18$) with CO_2 : Chromium cluster oxide bond energies

James B. Griffin and P. B. Armentrout

Department of Chemistry, University of Utah, Salt Lake City, Utah 84112

(Received 5 December 1997; accepted 11 February 1998)

The kinetic energy dependence of the reactions of Cr_n^+ ($n=1-18$) with CO_2 are studied in a guided ion beam mass spectrometer. The primary product ions are Cr_nO^+ , which then decompose by sequential loss of chromium atoms as the kinetic energy is increased. Simple collision-induced dissociation to form the Cr_{n-1}^+ product ions is also observed. Large cluster ions, $n \geq 9$, form the Cr_nCO_2^+ adduct at low kinetic energies. For many cluster sizes, the cross section for the primary reaction, $\text{Cr}_n^+ + \text{CO}_2 \rightarrow \text{Cr}_n\text{O}^+ + \text{CO}$, exhibits an interesting bimodal energy behavior that is discussed in some detail. $\text{Cr}_n^+ - \text{O}$ bond energies are measured and found to compare well with measurements obtained from guided ion beam studies of the $\text{Cr}_n^+ + \text{O}_2$ systems. The trends in this thermochemistry are discussed and compared to bulk phase oxidation values. © 1998 American Institute of Physics. [S0021-9606(98)02019-4]

I. INTRODUCTION

Oxidation of chromium is a subject of considerable interest because of its importance in preventing corrosion in iron based alloys.¹ Activation of CO_2 by transition metals is also of concern in the area of catalysis where CO_2 can be considered as an economical feedstock for chemical synthesis.² This is becoming increasingly important, as the reduction of CO_2 emissions is a problem of vast political and social implications because of its role in global warming. Gaining insight into the mechanisms and energetics of these oxidation and activation processes may therefore be of technological value, as well as being of fundamental interest.

One microscopic approach is to examine reactions with size specific clusters; however, the reactions of chromium clusters have not received as much attention as other transition metal clusters. Reactions of chromium clusters with O_2 have been studied by few groups.^{3,4} In our accompanying study of the reactivity of chromium cluster cations with oxygen, $\text{Cr}_n^+ + \text{O}_2$ ($n=2-18$),⁴ we found that the complexity of the reactions increased rapidly with cluster size up to about Cr_5^+ . For larger clusters, the product distribution and energy dependences were similar. Bond energies for the cluster monoxide and dioxide cations were reported and were compared to bulk phase chemistry. To verify some of the thermochemistry measured in this work, we chose to examine the reactions of these same chromium cluster cations with carbon dioxide. CO_2 was chosen for this study because it acts as an effective donor of a single oxygen atom thanks to the very strong CO bond energy. At present, there are no other published studies on the interaction of chromium clusters with CO_2 that we are aware of.

The reactivity of CO_2 has been studied on several metal surfaces,⁵ although there are no studies with a chromium surface that we are aware of. It was found that CO_2 will physisorb to most of the surfaces studied but chemisorption is less likely for many metals. For some of these reactive surfaces, a bimodal temperature dependence was observed

and shown to be related to formation of physisorbed and chemisorbed CO_2 . The physisorbed orientation has been assigned as having a linear structure, whereas the chemisorbed species has been assigned to bent anionic form, CO_2^- , which is a precursor for CO_2 dissociation.⁶

In the present work, we examine the reactions of chromium cluster cations, Cr_n^+ ($n=1-18$) with carbon dioxide. By analyzing the kinetic energy dependence of these processes, we are able to obtain quantitative data regarding the thermodynamics of the oxidation reactions. The trends in this information are discussed in some detail and compared with bulk phase thermochemistry and results derived from our concurrent study of chromium cluster cations reacting with oxygen.⁴ A key to this analysis is the availability of quantitative thermochemistry regarding the stability of the bare chromium clusters, previously measured in our laboratories.⁷ Further, this study provides a continuation of our previous work on the reactivity of transition metal cluster cations with various neutral gases.^{4,8-11}

II. EXPERIMENT

A. Instrumental

The ion beam apparatus and experimental techniques used in this work have been described in detail elsewhere.¹² Details for the generation of chromium cluster cations is described in full in the accompanying paper.⁴ In this study, reactions take place within a radio frequency (rf) octopole ion beam guide where the neutral gas (CO_2) is introduced. The quadrupole mass filter used to analyze the product ions has a mass limit of about 1100 amu such that chromium cluster reaction products up to $\text{Cr}_{18}\text{CO}_2^+$ can be studied. Absolute cross sections measured in our laboratory have an uncertainty estimated as $\pm 30\%$ and relative uncertainties of $\pm 5\%$. The uncertainty in the absolute energy scale is ± 0.05 eV (lab) and the widths range from 0.7 to 2.3 eV.

B. Threshold analysis

The threshold analysis procedure for the transition metal cluster reactivity studies has been described in detail in previous work.^{4,8,9} Briefly, the energy dependence of cross sections for endothermic processes in the threshold region is modeled using Eq. (1),

$$\sigma(E) = \sigma_0 \sum g_i (E + E_i + E_{\text{rot}} - E_0)^N / E, \quad (1)$$

where σ_0 is an energy independent scaling parameter, N is an adjustable parameter, E is the relative kinetic energy, E_{rot} is the average rotational energy of the cluster ion at 300 K, and E_0 is the threshold for the reaction at 0 K. The summation is over the vibrational states i having energies E_i and populations g_i , where $\sum g_i = 1$. We assume that the relative reactivity, as reflected by σ_0 and N , is the same for all vibrational states. The Beyer–Swinehart algorithm¹³ is used to evaluate the density of the ion vibrational states, and then the relative populations, g_i , are calculated by the appropriate Maxwell–Boltzmann distribution at 300 K. Vibrational frequencies for the bare cluster ions are obtained as outlined elsewhere,^{7,14} by using a Debye model suggested by Jarrold and Bower.¹⁵ Equation (1) has been used successfully in reproducing the cross sections of various ion–molecule reactions¹⁶ as well as collision induced dissociation (CID) and reaction processes of transition metal cluster ions.

Before comparing the model with the experimental data, several effects are taken into consideration. First, the thermal motion of the target gas and the kinetic energy distribution of the parent ion beam are both convoluted into Eq. (1) as described previously.¹⁷ Second, we account for the possibility that the processes being modeled occur more slowly than the experimental time window available, $\sim 10^{-4}$ s in our apparatus. This is achieved by incorporating Rice–Ramsperger–Kassel–Marcus (RRKM) theory into Eq. (1) as outlined elsewhere.¹⁸ All threshold analyses using Eq. (1) discussed below include this lifetime analysis. For these calculations, the transition state (TS) and its molecular constants are chosen as described in our previous work on the reactions of Fe_n^+ with CO_2 .⁹ We believe that the most reasonable choice places the TS at the point where the last species (CO or a chromium atom) is lost from the oxygenated cluster. This presumes that dissociation of the atoms lost prior to this event are facile and occur much more rapidly than this final atom loss step, a reasonable approximation as discussed previously.^{4,8,9} We also assume that the TS is a loose one, having molecular constants similar to the dissociated products. Most of the vibrational frequencies are chosen to equal those of the products, while the transitional modes (those turning into translations and rotations of the products) are chosen as outlined in recent work.^{19,20}

III. RESULTS

In all systems, the reactions were carried out from thermal energies to 10 eV or more in the center-of-mass frame. As a general nomenclature, we will refer to Cr_mO^+ products as “cluster monoxides,” and Cr_m^+ products as “cluster frag-

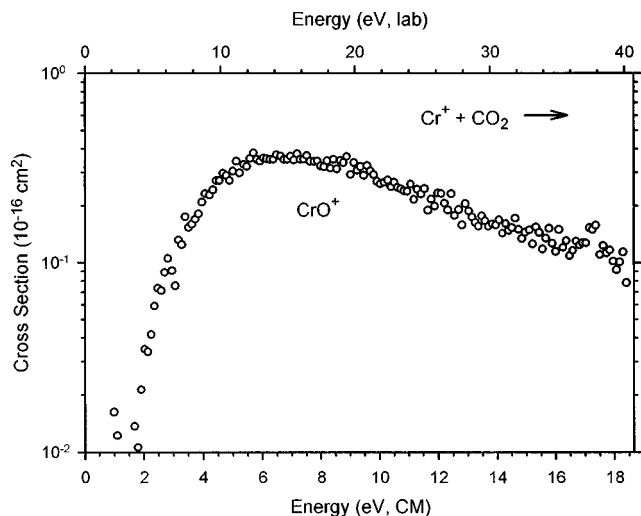


FIG. 1. Cross sections for the reaction of Cr^+ with CO_2 as a function of collision energy in the center-of-mass (lower x axis) and laboratory (upper x axis) frames.

ments,” where $m \leq n$ for reaction of Cr_n^+ . A complete set of figures for all Cr_n^+ clusters ($n = 1 - 18$) reacting with CO_2 can be obtained from Ref. 21.

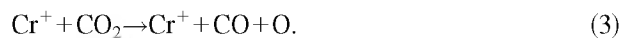
The dependence of the magnitudes of the product cross sections on the pressure of the neutral reagent was carefully checked. All products shown can be attributed to single collisions between the Cr_n^+ and CO_2 reactants with magnitudes representative of low pressure conditions. As the pressure of the CO_2 reactant was raised, exothermically formed Cr_nO^+ products react to yield Cr_mO_m^+ where m ranged from 2 to 4 or 5. Such products are not shown in Figs. 1–7 or Ref. 21 because they are clearly due to secondary reactions.

A. $\text{Cr}^+ + \text{CO}_2$

Chromium monomer ions react with CO_2 to form one product in reaction (2),



Other products, such as CrCO^+ , CrO_2^+ , and CrC^+ , were looked for but not observed. The cross section for process (2) is shown in Fig. 1. The CrO^+ product displays a single featured cross section with an apparent threshold near 1.8 eV and a maximum magnitude of about 0.36 \AA^2 at 6–8 eV. The cross section begins to decline at approximately the dissociation energy of CO_2 in the overall reaction (3),



The bond energies of CO_2 ($5.453 \pm 0.002 \text{ eV}$)²² and CrO^+ ($3.72 \pm 0.12 \text{ eV}$)²³ are well established. Thus, processes (2) and (3) have endothermicities of 1.73 ± 0.12 and $5.453 \pm 0.002 \text{ eV}$, respectively, which are in good agreement with what we observe. This shows that the laser vaporization/supersonic expansion produces only Cr^+ in its ^6S ground state.

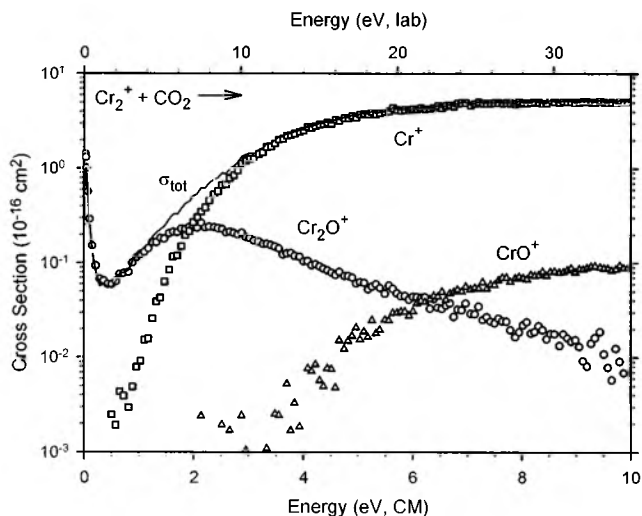


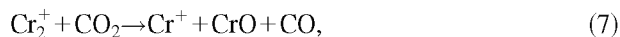
FIG. 2. Cross sections for the reaction of Cr_2^+ with CO_2 as a function of collision energy in the center-of-mass (lower x axis) and laboratory (upper x axis) frames.

B. $\text{Cr}_2^+ + \text{CO}_2$

Addition of a second Cr atom to the reactant cluster ion greatly increases the complexity of the reaction with CO_2 , as shown in Fig. 2. Three ionic products are now observed and can be identified by reactions (4)–(6),



The formation of Cr_2O^+ is the lowest energy product and displays both an exothermic and an endothermic feature in its cross section. This behavior is also observed in the reactions of Fe_n^+ with CO_2 but only for $n > 3$.⁹ The Cr^+ cross section is single featured and its cross section rises from a threshold of about 1 eV, consistent with simple CID, reaction (5), which can begin at 1.3 eV. Concomitant formation of CrO through reaction (7),



is endothermic by 2.24 ± 0.16 eV and there is no obvious evidence for this process. Cr^+ is the dominant product from about 2 eV to the highest energy studied and reaches a magnitude of 5 \AA^2 . This is about one-half the magnitude observed in the CID of Cr_2^+ with xenon.⁷ CrO^+ is formed through reaction (6) with an apparent threshold of about 3 eV, in agreement with the thermodynamic threshold of 3.03 ± 0.13 eV.

C. $\text{Cr}_3^+ + \text{CO}_2$

Results for the trimer chromium cation reacting with CO_2 are shown in Fig. 3. Products include metal fragments, Cr_2^+ and Cr^+ , and cluster monoxides, $\text{Cr}_{n-x}\text{O}^+$, $x = 0-2$. The metal fragments Cr^+ and Cr_2^+ have cross sections that rise from thresholds consistent with simple CID to $\text{Cr}^+ + \text{Cr}_2$ at 1.88 ± 0.10 and to $\text{Cr} + \text{Cr}_2^+$ at 2.01 ± 0.06 eV, respectively.⁷ The shape and magnitudes of these two products are very

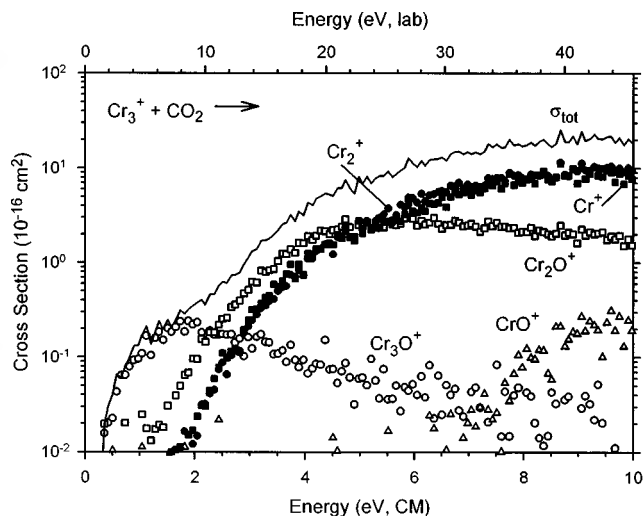


FIG. 3. Cross sections for the reaction of Cr_3^+ with CO_2 as a function of collision energy in the center-of-mass (lower x axis) and laboratory (upper x axis) frames.

similar, consistent with the intimate coupling between these two channels and the comparable ionization energies, (IE) (Cr_2) = 6.89 ± 0.08 ²⁴ and IE (Cr) = 6.766 eV.²² Although the magnitudes of these processes are comparable to those observed in the CID of Cr_3^+ with Xe,⁷ there, the Cr_2^+ product was favored by a factor of 3–4 at higher energies.

Both metal cluster fragments reach a magnitude of 10 \AA^2 and dominate the spectrum from 6 to 10 eV. Thus, efficient production of Cr_2^+ and Cr^+ accompanied by neutral products other than CO_2 and Cr or Cr_2 , respectively, are not indicated. For instance, formation of $\text{Cr}_2^+ + \text{Cr} + \text{CO}_2$ is 0.95 ± 0.10 eV more stable than $\text{Cr}_2^+ + \text{CrO} + \text{CO}$, making the latter products an unlikely reaction pathway, although contributions from alternative pathways cannot be eliminated at higher energies. Formation of $\text{Cr}^+ + \text{CrO} + \text{Cr} + \text{CO}$, a known decomposition path of the Cr_2O^+ product,⁴ can begin at 4.25 ± 0.18 eV and may contribute to the observed Cr^+ signal.

The cluster monoxide product ion formed at the lowest energy is Cr_3O^+ , produced in reaction (8),



This product ion can decompose to $\text{Cr}_2\text{O}^+ + \text{Cr}$ at slightly higher energies. The observation that the Cr_3O^+ cross section reaches a maximum near the threshold for Cr_2O^+ formation confirms this pathway. At still higher energies, Cr_2O^+ can decompose to $\text{Cr}^+ + \text{CrO}$ beginning at 4.25 ± 0.18 eV or to $\text{CrO}^+ + \text{Cr}$ beginning at 5.04 ± 0.17 eV. The larger endothermicity of the latter pathway explains the small size of the cross section for the CrO^+ product.

D. $\text{Cr}_n^+ + \text{CO}_2$ ($n = 4-18$)

Figures 4–7, which are typical of the results in the size range of $n = 4-18$, illustrate the reaction cross sections for Cr_4^+ , Cr_9^+ , Cr_{14}^+ , and Cr_{16}^+ reacting with CO_2 , respectively. These cluster sizes were chosen because there are noticeable differences in the observed reactivity at these points. There are only three types of products formed in these reactions:

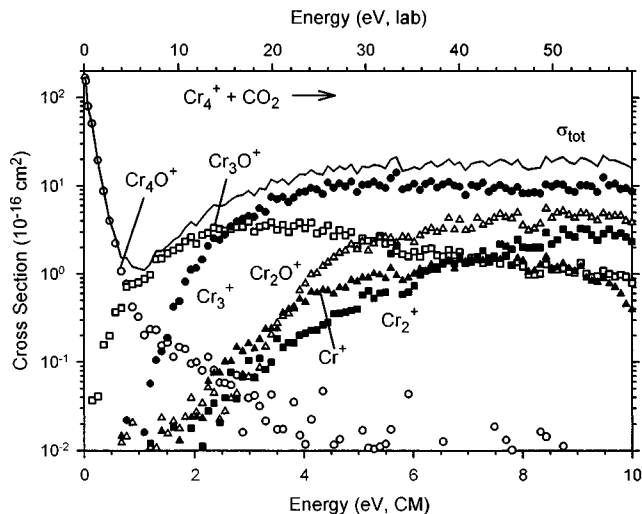


FIG. 4. Cross sections for the reaction of Cr_4^+ with CO_2 as a function of collision energy in the center-of-mass (lower x axis) and laboratory (upper x axis) frames.

cluster monoxides, $\text{Cr}_{n-x}\text{O}^+$; cluster fragments, Cr_{n-x}^+ ; and adducts, Cr_nCO_2^+ , which are observed only for $n \geq 9$.

The dominant products at the lowest energies from $n=1-13$ are the Cr_nO^+ ions, formed in reaction (9),



For clusters in the range $n=4-6$, the cross sections for this reaction decline with increasing energy, typical behavior for barrierless exothermic reactions. This exothermic feature displays a magnitude near 200 \AA^2 at subthermal energies for these cluster sizes. This is close to 100% of the magnitude predicted by the Langevin-Gioumousis-Stevenson cross section model (LGS),²⁵ $\sigma_{\text{LGS}} = \pi e(2\alpha/E)^{1/2}$, where α is the polarizability of CO_2 (2.59 \AA^3).²⁶ At 0.02 eV, σ_{LGS} is about 192 \AA^2 . The endothermic portion of this process, compared with those in Cr_n^+ ($n=1-3$ and $7-18$) and in the analogous reaction of all Fe_n^+ ($n=1-18$),⁹ contribute little to the

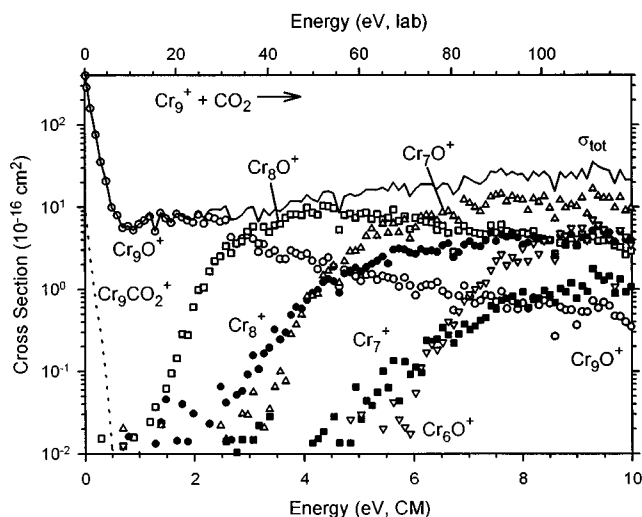


FIG. 5. Cross sections for the reaction of Cr_9^+ with CO_2 as a function of collision energy in the center-of-mass (lower x axis) and laboratory (upper x axis) frames.

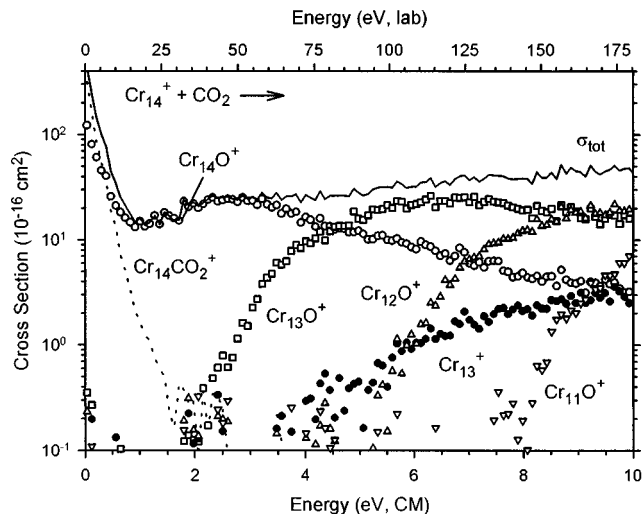


FIG. 6. Cross sections for the reaction of Cr_{14}^+ with CO_2 as a function of collision energy in the center-of-mass (lower x axis) and laboratory (upper x axis) frames.

Cr_nO^+ cross section. For cluster sizes $n=7-15$, the cross sections for reaction (9) display two features. The exothermic features have magnitudes that increase from $n=7-10$ and then decrease from $n=10-18$ (reaching a maximum at $n=10$ at about 320 \AA^2). The endothermic features rise from apparent thresholds of about 1 eV, similar to Cr_2^+ . When $n=16$ and 17, the exothermic portion disappears and there exists only an endothermic cross section that rises from a threshold of about 0.5 eV. Cr_{18}^+ then displays a two featured cross section again, but the exothermic portion is much smaller (about 5 \AA^2) than the other clusters that display both features.

As discussed in our previous work on the reactions of Fe_n^+ with CO_2 ,⁹ bimodal behavior that we observe is unusual because such features can often be related to separate reaction pathways associated with different neutral products for the same ionic product. However, formation of Cr_nO^+ has

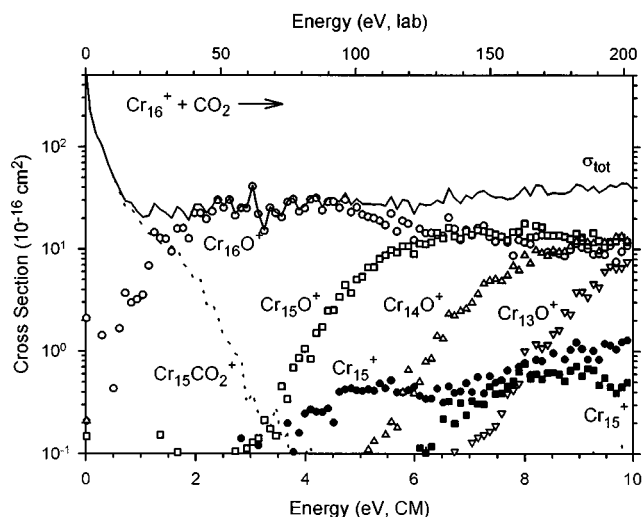


FIG. 7. Cross sections for the reaction of Cr_{17}^+ with CO_2 as a function of collision energy in the center-of-mass (lower x axis) and laboratory (upper x axis) frames.

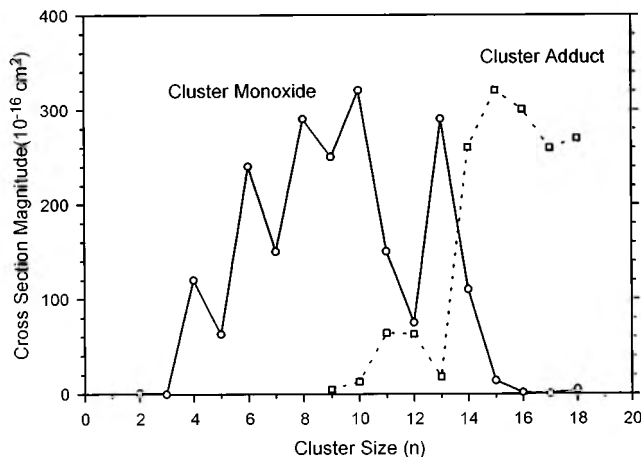


FIG. 8. Comparison of the magnitudes of the cluster-oxide and cluster adduct cross sections at an energy of ~ 0.05 eV as a function of number of atoms in the Cr_n^+ reactant.

only one possible pathway that is thermodynamically viable, reaction (9), because the CO bond strength is so high, 11.1 eV.²⁷ To check whether these multiple features could possibly be due to artifacts, several diagnostic reactions were run. Contamination of the neutral reactant with O_2 or H_2O is plausible and could lead to the Cr_nO^+ products. Results from our study of the reactions of chromium cluster ions with molecular oxygen⁴ indicate that if O_2 were present, we would observe intense cluster dioxide products formed under single collision conditions. Such products were observed only as secondary reaction products in minor amounts in the present work. To remove traces of water from the sample gas, we subjected the reactant CO_2 gas to several cycles of drying on liquid nitrogen cooled molecular sieves. This treatment had no effect on the appearance of the cross sections. Possible effects of multiple collisions were checked carefully to assure that both features in the Cr_nO^+ cross sections are the result of a single collision between the cluster ion and CO_2 . The possibility of internally excited cluster ions was ruled out by examining the reaction of these ions with O_2 and determining that the monoxide product ions in this system displayed only a single featured, endothermic cross section. CID studies were also performed to confirm that the clusters fragment with the same energetics as in previous studies.⁷ Thus, we conclude that the dual features in the Cr_nO^+ cross sections observed are real. An explanation for such features is discussed below.

Results for reactions of Cr_n^+ ($n=9-14$) with CO_2 illustrate that the magnitude of the adduct product ion, Cr_nCO_2^+ , and the low energy monoxide product, Cr_nO^+ , varies considerably with cluster size. Figure 8 shows the cross section magnitude of the cluster adduct and cluster monoxide at about 0.05 eV as a function of the number of Cr atoms in the cluster. A few features in this figure are particularly interesting. First, the intensity oscillation of the cluster monoxide is inversely correlated to the oscillations that we observe in our studies on the stabilities of the bare chromium clusters.⁷ Second, we note that the magnitude of the adduct cross section and that of the Cr_nO^+ cross section are inversely correlated. These cluster products show a remarkable size dependent

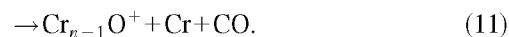
reactivity that was not observed in our studies of Cr_n^+ reacting with O_2 .⁴

As the energy is raised, the primary Cr_nO^+ products begin to decompose by sequential loss of chromium atoms. This is apparent from the observation that the Cr_mO^+ product cross section reaches a maximum at an energy near the onset for the $\text{Cr}_{m-1}\text{O}^+$ cross section. Formation of cluster fragment ions appears to be exclusively by simple CID processes. These become increasingly inefficient as the cluster size increases. For $n=2-11$ clusters, the cross sections for the CID process in these reactions are about equal or slightly smaller than those measured in the $\text{Cr}_n^+ + \text{Xe}$ system.⁷ For clusters $n > 11$, the CID processes observed here are about an order of magnitude smaller than those seen in the Xe system.⁷

IV. DISCUSSION

A. Cr_nO^+ bond energies

Based on the bond energies for $\text{Cr}_n^+ - \text{O}$ measured in the accompanying paper on the reactions of chromium cluster cations with O_2 ,⁴ reaction (9) is exothermic for all clusters except the monomer and trimer (possibly thermoneutral for $n=18$). Therefore, the endothermic features in the Cr_nO^+ cross sections do not provide direct thermodynamic information regarding the Cr_nO^+ bond energies. Therefore, we turn to an examination of the $\text{Cr}_{n-1}\text{O}^+$ products which are formed by subsequent Cr atom dissociation from the primary products. Bond energies for $\text{Cr}_{n-1}^+ - \text{O}$ can be measured by determining the difference between the thresholds for reactions (10) and (11),



Specifically, the bond energies are calculated using Eq. (12),

$$D(\text{Cr}_{n-1}^+ - \text{O}) = E_0(10) - E_0(11) + D(\text{O}-\text{CO}). \quad (12)$$

The thresholds for reactions (10) are equivalent to the bond energies of the bare chromium cluster ions, $D(\text{Cr}_{n-1}^+ - \text{Cr})$, and have been measured previously.⁷ We also verified that the present data for reaction (10) can be reproduced by Eq. (1) using the previously published values of $D(\text{Cr}_{n-1}^+ - \text{Cr})$ along with reasonable N values. Here, we determine the thresholds for reactions (11) using an analysis with Eq. (1) as outlined above. The optimized parameters of this model are listed in Table I, while Table II lists the bond dissociation energies of $\text{Cr}_n^+ - \text{O}$ obtained from these thresholds calculated using Eq. (12).

The reliability of thermochemistry determined from these thresholds is limited somewhat by the second order character of these reactions, corresponding to loss of $\text{Cr} + \text{CO}$ from the initially formed Cr_nCO_2^+ intermediate. An additional drawback to measuring thermochemistry in this manner is that the uncertainty is larger because it includes the uncertainties of both reactions (10) and (11). A redeeming feature, however, is that the errors due to the kinetic shifts and internal energies should be reduced because identical assumptions are employed for both threshold measurements.

TABLE I. Summary of parameters used in Eq. (1) for the analysis of cross sections for $\text{Cr}_n^+ + \text{CO}_2 \rightarrow \text{Cr}_{n-1}\text{O}^+ + \text{Cr} + \text{CO}$.

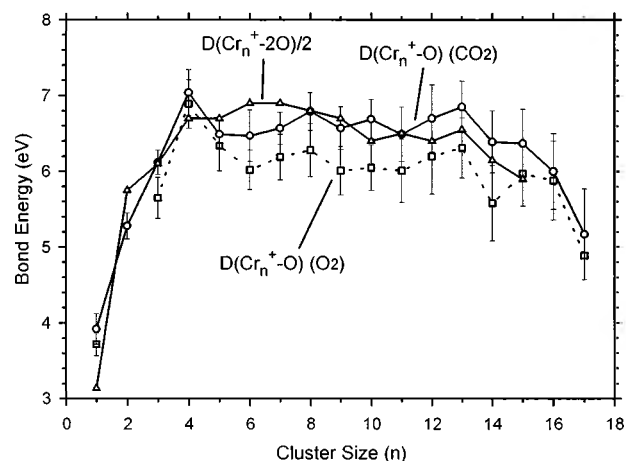
n	σ_0	N	E_0 , eV
1 ^a	0.28	1.5(0.2)	1.79(0.12)
3	2.4	1.9(0.2)	1.84(0.26)
4	1.9	2.0(0.3)	0.44(0.12)
5	1.9	1.8(0.3)	0.76(0.18)
6	4.2	2.0(0.3)	0.75(0.15)
7	8.7	1.8(0.3)	1.58(0.13)
8	11.4	1.5(0.3)	1.25(0.17)
9	6.2	2.3(0.3)	1.27(0.20)
10	7.1	2.3(0.3)	1.34(0.20)
11	7.8	2.0(0.3)	1.30(0.22)
12	2.9	2.5(0.3)	1.65(0.24)
13	1.4	2.0(0.3)	1.90(0.24)
14	2.4	1.8(0.3)	1.71(0.28)
15	13.9	2.0(0.3)	1.89(0.27)
16	11.9	1.8(0.3)	2.05(0.28)
17	14.7	2.0(0.3)	2.21(0.28)
18	21.7	1.8(0.3)	2.30(0.31)

^aFor $\text{Cr}^+ + \text{CO}_2 \rightarrow \text{CrO}^+ + \text{CO}$.

Figure 9 shows the $\text{Cr}_n^+ - \text{O}$ bond energies determined here as a function of cluster size along with values derived from our study of the reactions of Cr_n^+ with O_2 .⁴ The agreement is within experimental uncertainty with the exception of a few cases, namely $n=3, 7, 9$, and 10 . However, we note that the values obtained here are generally larger than those measured for the monoxides from the reaction with O_2 . This difference is easily observed in a direct comparison of the data for the two systems. The thermodynamic threshold for the reaction of Cr_n^+ with dioxygen, $D(\text{O}_2) = 5.115$ eV, is 0.34 eV lower than that for the reaction with CO_2 , $D(\text{O}-\text{CO}) = 5.453$ eV. However, we observe that the thresholds for production of $\text{Cr}_{n-1}\text{O}^+$ in the CO_2 system are generally lower in energy than those for the O_2 system. This probably indicates that the thresholds in the reaction with O_2

TABLE II. Bond energies for $\text{Cr}_n^+ - \text{O}$ from this study and the reaction of Cr_n^+ with O_2 .

n	$D(\text{Cr}_n^+ - \text{O})$ (eV) ^a	$D(\text{Cr}_n^+ - \text{O})$ (eV) ^b
1	3.72(0.15) ^c	3.66(0.20)
2	NA	5.62(0.27)
3	4.94(0.27)	6.05(0.16)
4	6.78(0.32)	6.93(0.30)
5	6.34(0.33)	6.37(0.18)
6	5.98(0.26)	6.42(0.34)
7	5.73(0.30)	6.45(0.21)
8	6.25(0.35)	6.76(0.25)
9	5.89(0.32)	6.51(0.28)
10	6.08(0.30)	6.72(0.26)
11	5.98(0.42)	6.47(0.36)
12	6.03(0.50)	6.55(0.44)
13	6.25(0.40)	6.80(0.34)
14	5.52(0.50)	6.33(0.41)
15	5.93(0.52)	6.32(0.45)
16	5.95(0.52)	5.98(0.50)
17	5.04(0.80)	5.31(0.60)

^aFrom Ref. 4.^bThis study measured from $\text{Cr}_n^+ + \text{CO}_2 \rightarrow \text{Cr}_{n-1}\text{O}^+ + \text{Cr} + \text{CO}$.^cFrom Ref. 23.FIG. 9. Comparison of the $\text{Cr}_n^+ - \text{O}$ bond energies measured in this study to $D(\text{Cr}_n^+ - 2\text{O})/2$ and $D(\text{Cr}_n^+ - \text{O})$ measured in previous work on the reactions of $\text{Cr}_n^+ + \text{O}_2$ (Ref. 2) as a function of cluster size n .

are shifted slightly to higher energies due to competition with the much more favorable $\text{Cr}_{n-x}\text{O}_2^+$ products. Thus, the bond energies determined in the present study are believed to be somewhat more reliable than those from our O_2 study.

Figure 9 also compares the bond energies obtained in this system with those measured from the thresholds and relative energies of the dioxygenated Cr_nO_2^+ products formed in the reaction of Cr_n^+ with dioxygen.⁴ These bond energies are for $\text{Cr}_n^+ - (\text{O})_2$ and hence are divided by two to compare to the $\text{Cr}_n^+ - \text{O}$ bond energies. For these bond energies to agree exactly, both oxygens in Cr_nO_2^+ would have to be bound to the cluster with identical bond energies, which need not be correct. Although there do appear to be some systematic deviations (the $\text{Cr}_n\text{O}_2^+/2$ bond energies are larger than those for $n=5-7$ and smaller for $n=12-15$), the bond energies are within the combined experimental error bars for all clusters. Overall, this comparison suggests that the first and second oxygen atoms bind similarly to chromium cluster cations and lends some support to the accuracy of the numbers in both studies.

B. Trends in oxygenated chromium cluster stability

Another way to examine the trends in this thermochemistry is to compare the stabilities of bare and oxygenated cluster ions with regard to loss of a chromium atom, the lowest energy dissociation process in all cases. The $\text{OCr}_{n-1}^+ - \text{Cr}$ bond energies are calculated from Eq. (13),

$$D(\text{OCr}_{n-1}^+ - \text{Cr}) = D[\text{Cr}_n^+ - \text{O}] - D[\text{Cr}_{n-1}^+ - \text{O}] + D(\text{Cr}_{n-1}^+ - \text{Cr}), \quad (13)$$

where the required bond energies are taken from Table II and Ref. 7. These comparisons are shown in Fig. 10. In general, oxidation of the clusters does not change their stability with respect to chromium atom evaporation by an appreciable amount for clusters $n > 5$. This may simply mean that chromium atom loss occurs at sites remote from the oxygen atom bonding. For clusters $n=2-4$, oxidation increases the stability. The easiest explanation is that the oxygen is bound in bridging sites to several of the metal atoms, thereby holding

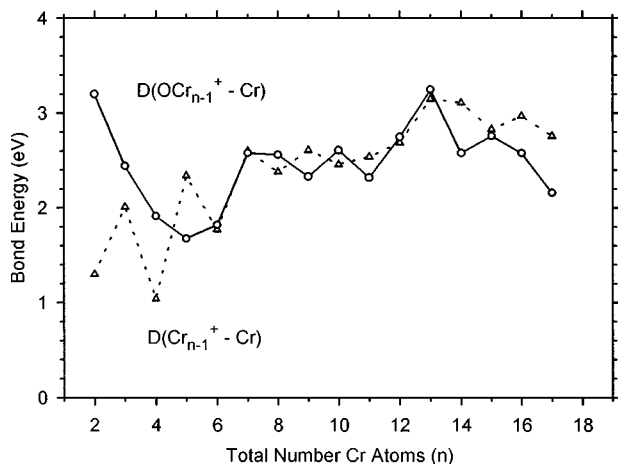


FIG. 10. Comparison of the $D(\text{OCr}_{n-1}^+ - \text{Cr})$ bond energy calculated using Eq. (13) to the CID bond energies (from Ref. 7) as a function of the cluster size n .

the cluster together more tightly. However, it is conceivable that a terminally bound oxygen atom could accomplish this through an electronic effect. Interestingly, the Cr_5O^+ cluster is less stable than the bare Cr_5^+ cluster. (This might also be true of $n=14, 16,$ and 17 , although the uncertainties in the bond energies for these clusters makes this conclusion less secure.) In this case, this is most easily attributed to the enhanced stability of the Cr_4O^+ cluster relative to Cr_5O^+ compared to the stability of Cr_4^+ and Cr_5^+ .

C. Reaction mechanism

The only processes observed in the interactions of chromium cluster cations with carbon dioxide are CID and cluster oxidation with elimination of CO. Products observed at high energies are simply due to further dissociation (by Cr atom loss) of the products formed by these two primary channels. Adducts of the clusters with CO_2 are observed only for clusters with $n \geq 9$.

The probability of the cluster oxidation reaction at thermal energies is plotted in Fig. 8. The strong oscillations in this plot are directly correlated with the stability of the bare clusters up through $n=10$. As noted in our previous CID study,⁷ odd-sized cluster cations are found to be more stable than even-sized cluster cations (Fig. 10). This was postulated to be because the odd-sized clusters had an even number of $4s$ electrons and thus could be closed-shell in the outermost frontier orbitals, while the even-sized clusters had an odd number of $4s$ electrons, thereby giving them radical character. Note that these even-sized clusters are the more reactive ones, consistent with our previous assignments.

Because no products containing carbon, with the exception of the adducts, are observed, there is no direct experimental evidence that distinguishes between oxidation reactions that occur by a dissociative chemisorption process that form a transient $\text{O}-\text{Cr}_n^+-\text{CO}$ intermediate from ones that occur by direct oxygen atom abstraction. However, because Cr_nO^+ formation is exothermic in all cases but $n=1$, dissociative chemisorption is likely to be lower energy process

than physisorption of an intact CO_2 molecule. This is further indicated by noting that atomic metal ion bonds to CO are generally stronger than those to CO_2 .²⁸

Another indication of this is the inverse correlation between the magnitudes of the low energy feature in the Cr_nO^+ cross section and the Cr_nCO_2^+ adduct cross section (Fig. 8). Clearly, large clusters are needed to observe the adduct. This can be explained if excess energy released during the exothermic dissociative chemisorption process is dissipated in a large cluster such that the lifetime of the OCr_nCO^+ intermediate is long enough that this species can travel through our instrument and be detected. For smaller clusters and the more reactive medium-sized clusters, CO loss is rapid and efficient, consistent with a relatively weak Cr^+-CO bond energy of 0.93 eV ²⁹ compared to that of Cr^+-O . For the less reactive medium-sized clusters, the lifetime of this transient intermediate is apparently similar to the experimental flight time of the ions.

The most interesting observation in this reaction system is the disparate behavior of the Cr_nO^+ product cross sections. Clusters $n=2$ and $7-15$ display both obvious exothermic and endothermic features. Clusters $n=1, 3, 16,$ and 17 exhibit no obvious exothermic features, while $n=4-6$ have no obvious endothermic features. Dual features in the analogous product cross sections were also observed in the reaction of Fe_n^+ with CO_2 .⁹ There, we reasoned that there are two possible explanations for these two features. The first explanation starts by noting that $\text{CO}_2(^1\Sigma_g^+)$ does not diabatically dissociate to ground state $\text{CO}(^1\Sigma_g^+) + \text{O}(^3P)$, but rather to $\text{CO}(^1\Sigma_g^+) + \text{O}(^1D)$, 1.97 eV higher in energy. Reactions of the iron monomer and dimer cations had thresholds that correlated nicely with thresholds calculated for this spin-allowed (diabatic) dissociation channel. Therefore, we assigned the exothermic feature to reaction along the adiabatic potential energy surface and the endothermic feature to reaction along the diabatic pathway.

This explanation is also feasible in the present system. This would suggest that the observation of one or both features in the cross sections could be attributed to the spin states of the clusters and how well they correlate with the states of the oxygenated clusters. There is less direct evidence for such a proposal in the present system because the reaction of the monomer with CO_2 gives a threshold that is consistent with a reaction along the adiabatic potential energy surface, i.e., the measured threshold (Table I) is consistent with the value $1.73 \pm 0.12 \text{ eV}$ calculated using known thermochemistry $D_0(\text{Cr}^+-\text{O}) = 3.72 \pm 0.12$ (Ref. 23) and the adiabatic dissociation energy $\text{CO}(^1\Sigma_g^+) + \text{O}(^3P)$, $D_0(\text{OC}-\text{O}) = 5.453 \pm 0.002$.²² Further, the dimer displays the double featured cross section for the formation of CrO^+ so that no elevated thresholds are observed in the present system, in contrast to the observations for iron clusters.

A second possible explanation for the two features is a direct and indirect (resonant or trapping mediated) process. Such behavior has been observed and described experimentally for the reactions of alkanes with iridium surfaces³⁰ and theoretically for the reactions of nickel clusters with D_2 .³¹ This hypothesis suggests that at low energies, there is a long lifetime for the transient Cr_nCO_2^+ intermediate where the

CO₂ is physisorbed on the cluster. At these energies, there is sufficient time for the CO₂ molecule to find an optimum site on the cluster for activation of the C–O bond, leading to dissociative chemisorption. As the energy increases, the lifetime of the intermediate decreases, thereby limiting the efficiency of this indirect process. At still higher energies, the reactions can occur by a direct mechanism which has an apparent threshold. This apparent threshold could represent the barriers to chemisorption at sites that are more abundant on the cluster or it could be a dynamic barrier where chemisorption occurs without relaxation of the cluster necessary to access the lowest energy pathway. (It should be noted that similar effects could also be involved for the first mechanism involving electronic factors discussed above.) This mechanism was discounted in the iron system, although the evidence against it was indirect. In the present work, there is no evidence to support or discount it.

D. Comparison to bulk phase thermochemistry

Ideally, we would like to compare the bond energies determined here to those on bulk phase Cr surfaces. Unfortunately, the only information available on the reaction of CO₂ with chromium surfaces is the adsorption onto polycrystalline films where the heat of adsorption is 70 kcal/mol.³² This involves the complete dissociation of CO₂ and does not yield any useful information for comparison since CO is not bound to the clusters. However, we can compare the surface–oxygen bond energy with those measured in this system. The details of this comparison are discussed in the accompanying paper on O₂ reactions.⁴ The metal surface–oxygen bond energy is 6.4 ± 0.2 eV,³² comparable to our average cluster–oxygen bond energy of 6.43 ± 0.44 eV.⁴ Thus, the thermochemistry obtained here for small chromium clusters is comparable to that for bulk phase chromium. This suggests that the use of clusters to model the reactivity at surface defects, at least for oxygen, may be reasonable.³³

Complete dissociation of the CO₂ molecule does not occur on chromium clusters as shown by the lack of any carbide products except at high energies for the dimer ion. However, similar to the surface reactivity, CO₂ does undergo dissociative chemisorption on chromium clusters as argued above. The important difference between cluster and surface systems is that the clusters have a discrete energy content, i.e., the sum of the internal energy in the cluster reactant and the excess energy deposited upon formation of the cluster–oxygen and cluster–carbonyl bonds. As more kinetic energy is added to the system, the internal energy of the cluster increases until the cluster CO bond is broken. This is the lowest energy process by which the Cr_nCO₂⁺ cluster can dispose of the excess energy (the most efficient cooling mechanism). We can infer that the bond energy of CO to the cluster must be much less than the energy to lose either a chromium atom or an oxygen atom because we see no cluster cation–CO products nor any CO₂ adducts where the cluster has fewer chromium atoms than the reactant. In the reaction of Cr_n⁺ + O₂, the cluster adduct behaves quite differently because the most efficient cooling mechanism is evaporation of Cr atoms. In addition, the Cr_nO₂⁺ adduct is observed over a

much wider range of energies than the Cr_nCO₂⁺ adduct, another clue that CO is bound more weakly to chromium cluster cations than O or Cr.

ACKNOWLEDGMENT

This work is supported by the Department of Energy, Office of Basic Energy Sciences.

- ¹F. P. Fehlner and M. J. Graham, in *Corrosion Mechanisms in Theory and Practice*, edited by P. Marcus and J. Odar (Marcel Dekker, New York, 1995), p. 136.
- ²S. J. Barer and K. M. Stern, in *Catalytic Activation of Carbon Dioxide*, edited by W. M. Ayers (American Chemical Society, Washington, D.C., 1988), p. 1.
- ³G. C. Nieman, E. K. Parks, S. C. Richtsmeier, K. Liu, L. G. Pobo, and S. J. Riley, *High. Temp. Sci.* **22**, 115 (1986).
- ⁴J. B. Griffin and P. B. Armentrout, *J. Chem. Phys.* **108**, 8062 (1998), preceding paper.
- ⁵Reviewed by J. Wambach and H.-J. Freund, in *Carbon Dioxide Chemistry: Environmental Issues*, edited by J. P. Pradier and C.-M. Pradier (Atheneum, U.K., 1994), p. 31.
- ⁶H. J. Freund, H. Behner, B. Bartos, G. Wedler, H. Kuhlenbeck, and M. Neumann, *Surf. Sci.* **180**, 550 (1987).
- ⁷C.-X. Su and P. B. Armentrout, *J. Chem. Phys.* **99**, 6506 (1993).
- ⁸J. B. Griffin and P. B. Armentrout, *J. Chem. Phys.* **106**, 4448 (1997).
- ⁹J. B. Griffin and P. B. Armentrout, *J. Chem. Phys.* **107**, 5345 (1997).
- ¹⁰J. Conceição, S. K. Loh, L. Lian, and P. B. Armentrout, *J. Chem. Phys.* **104**, 3976 (1996).
- ¹¹J. Xu, M. T. Rodgers, J. B. Griffin, and P. B. Armentrout, *J. Chem. Phys.* (submitted).
- ¹²S. K. Loh, L. Lian, and P. B. Armentrout, *J. Chem. Phys.* **91**, 6148 (1989).
- ¹³T. Beyer and D. F. Swinehart, *Commun. ACM* **16**, 379 (1973); S. E. Stein and B. S. Rabinovitch, *J. Chem. Phys.* **58**, 2438 (1973); *Chem. Phys. Lett.* **49**, 183 (1977); R. G. Gilbert and S. C. Smith, *Theory of Unimolecular and Recombination Reactions* (Blackwell Sci., Oxford, 1990).
- ¹⁴S. K. Loh, L. Lian, and P. B. Armentrout, *J. Chem. Phys.* **91**, 6148 (1989).
- ¹⁵M. F. Jarrold and J. E. Bower, *J. Chem. Phys.* **87**, 5728 (1987).
- ¹⁶J. L. Elkind and P. B. Armentrout; *J. Am. Chem. Soc.* **90**, 6576 (1986); P. B. Armentrout, *Int. Rev. Phys. Chem.* **9**, 115 (1990); in *Advances in Gas Phase Ion Chemistry*, edited by N. G. Adams and L. M. Babcock (JAI, Greenwich, 1992), Vol. I, p. 83; D. E. Clemmer, Y.-M. Chen, N. Aristov, and P. B. Armentrout, *J. Chem. Phys.* **98**, 7538 (1994).
- ¹⁷K. M. Ervin and P. B. Armentrout, *J. Chem. Phys.* **83**, 166 (1985).
- ¹⁸M. T. Rodgers, K. M. Ervin, and P. B. Armentrout, *J. Chem. Phys.* **106**, 4499 (1997).
- ¹⁹M. T. Rodgers and P. B. Armentrout, *J. Phys. Chem. A* **101**, 2614 (1997).
- ²⁰M. T. Rodgers and P. B. Armentrout, *J. Phys. Chem. A* **101**, 1238 (1997).
- ²¹See AIP document No. PAPS JCPA6-108-020819 for 18 pages of figures. Order by PAPS number and journal reference from American Institute of Physics, Physics Auxiliary Publication Service, Carolyn Gehlbach, 500 Sunnyside Boulevard, Woodbury, New York 11797-2999. Fax: 516-576-2223, e-mail: paps@aip.org. The price is \$1.50 for each microfiche (98 pages) or \$5.00 for photocopies of up to 30 pages, and \$0.15 for each additional page over 30 pages. Airmail additional. Make checks payable to the American Institute of Physics.
- ²²S. G. Lias, J. E. Bartmess, J. F. Liebman, J. L. Levin, R. D. Levin, and W. G. Mallard, *J. Phys. Chem. Ref. Data Suppl.* **17**, 1 (1988).
- ²³E. R. Fisher, J. L. Elkind, D. E. Clemmer, R. Georgiadis, S. K. Loh, N. Aristov, L. S. Sunderlin, and P. B. Armentrout, *J. Chem. Phys.* **93**, 2676 (1990).
- ²⁴C.-X. Su, D. A. Hales, and P. B. Armentrout, *Chem. Phys. Lett.* **201**, 2449 (1982).
- ²⁵G. Gioumoussis and D. P. Stevens, *J. Chem. Phys.* **29**, 294 (1958).
- ²⁶E. W. Rothe and R. B. Bernstein, *J. Chem. Phys.* **31**, 1619 (1959).
- ²⁷K. P. Huber and G. Herzberg, *Molecular Spectra and Molecular Structure IV. Constants of Diatomic Molecules* (Van Nostrand Reinhold, New York, 1979).
- ²⁸M. Sodupe, V. Branchadel, M. Rosi, and C. W. Bauschlicher, Jr., *J. Phys. Chem.* **101**, 7854 (1997), and references therein.

- ²⁹F. A. Khan, D. E. Clemmer, R. H. Schultz, and P. B. Armentrout, *J. Phys. Chem.* **97**, 7978 (1993).
- ³⁰W. Hago, D. Kelly, and W. H. Weinberg, *J. Vac. Sci. Technol. A* **14**, 1578 (1996); D. Kelly and W. H. Weinberg, *ibid.* **14**, 1588 (1996).
- ³¹J. Jellinek and Z. B. Güvenç, in *Topics in Atomic and Nuclear Collisions* (Plenum, New York, 1994); *Z. Phys. D* **26**, 114 (1993); in *Nuclear Physics Concepts in the Study of Atomic Cluster Physics* (Springer-Verlag, Berlin, 1991).
- ³²D. Brennan and D. O. Hayward, *Philos. Trans. R. Soc. London, Ser. A* **258**, 375 (1965).
- ³³G. Somorjai, *Chemistry in Two Dimensions: Surfaces* (Cornell University Press, Ithaca, 1981).